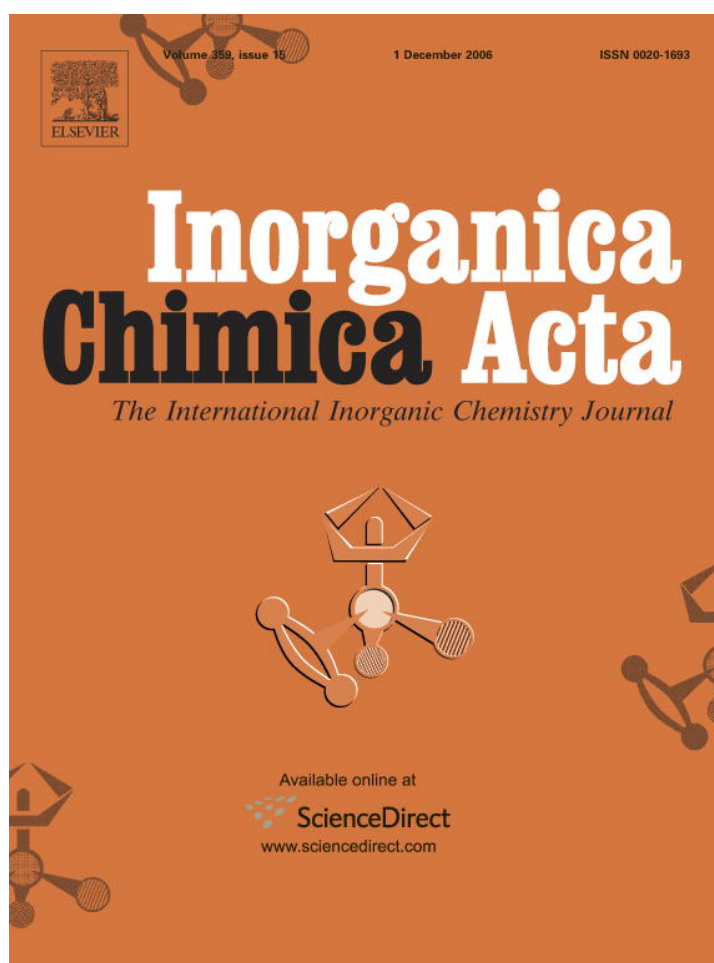


Provided for non-commercial research and educational use only.
Not for reproduction or distribution or commercial use.



This article was originally published in a journal published by Elsevier, and the attached copy is provided by Elsevier for the author's benefit and for the benefit of the author's institution, for non-commercial research and educational use including without limitation use in instruction at your institution, sending it to specific colleagues that you know, and providing a copy to your institution's administrator.

All other uses, reproduction and distribution, including without limitation commercial reprints, selling or licensing copies or access, or posting on open internet sites, your personal or institution's website or repository, are prohibited. For exceptions, permission may be sought for such use through Elsevier's permissions site at:

<http://www.elsevier.com/locate/permissionusematerial>



Synthesis, immobilization, and solid-state NMR of new phosphine linkers with long alkyl chains

Rachid Fetouaki, Annekathrin Seifert, Mona Bogza, Thomas Oeser, Janet Blümel *

Organisch-Chemisches Institut der Universität Heidelberg, Im Neuenheimer Feld 270, D-69120 Heidelberg, Germany

Received 29 June 2006; accepted 28 July 2006

Available online 11 August 2006

Dedicated to Professor Dr. Dr. h.c. mult. Wolfgang A. Herrmann in appreciation of his many contributions to organometallic chemistry and catalysis.

Abstract

Monodentate and chelating phosphines with long alkyl chains, incorporating ethoxy- or chlorosilane functions for immobilizations, have been synthesized and fully characterized. The new compounds $(\text{EtO})_3\text{Si}(\text{CH}_2)_x\text{PPh}_2$, $\text{Cl}_2\text{Si}(\text{CH}_2\text{CH}_2\text{PPh}_2)_2$, and $(\text{EtO})_2\text{Si}[(\text{CH}_2)_x\text{PPh}_2]_2$ ($x = 7, 11$) could be prepared in high yields from cheap starting materials, and they have been characterized by multinuclear NMR spectroscopy and X-ray crystallography. The phosphines have been immobilized on silica in a well-defined manner, and the modified silicas have been studied by ^{31}P and ^{29}Si solid-state NMR of the dry materials and of the suspensions.
© 2006 Elsevier B.V. All rights reserved.

Keywords: Ethoxysilanes; Chelating phosphines; Solid-state NMR; Immobilization; Linkers; Alkyl chains

1. Introduction

Whether immobilized species are successful or not is crucially dependent on the nature of the linker. This holds for combinatorial chemistry [1], solid-phase synthesis [2], chromatography [3], and catalysis alike [4]. Many groups [5], including us, have tried to improve the recyclability and lifetime of immobilized catalysts by tethering them on oxide supports by linkers [6–8]. For characterizing the resulting amorphous materials, as well as their surface chemistry, solid-state NMR spectroscopy [9] proves to be an indispensable and powerful analytical method. For our systems, we recently optimized the cross polarization (CP) process at high magic angle spinning (MAS) frequencies [10] for getting better signal to noise ratios (S/N), and implemented stationary [11a,11b] and HRMAS suspension NMR spectroscopy [11c] to study the mobilities of surface species, as well as their reactivity with oxide surfaces, and their structural nature [11c,11d].

Using our repertoire of different solid-state NMR techniques [10,11], we could clarify for example the reaction of the popular linker $\text{Ph}_2\text{P}(\text{CH}_2)_3\text{Si}(\text{OEt})_3$ and of related chelating phosphines with the silica surface [6–8,12,13]. The solvent was shown to be important for the immobilization process [14], while the strongest bonding takes place with silica [11b]. Furthermore, metal complexes with two monodentate linkers are not necessarily bound in a chelating manner [15], making even the linkers that are not anchored directly on the surface, but merely by coordination to the metal center, vulnerable to leaching [7c,11b]. This problem has been solved by using chelating linkers that prolong the lifetimes of the catalysts substantially [6,7,11c,12]. Nevertheless, chelate phosphine linkers incorporating ethoxysilane groups for immobilizations on silica are still rarely found in the literature [6–8,12,17], and many of them, e.g. bisphosphinoamine linkers [11c], even decompose during the immobilization process or form phosphonium salts as side products [11c,16].

In earlier studies on Ni, Rh, and Pd complexes, we have shown that dppe- and dppp-type chelate linkers lead to the

* Corresponding author. Tel.: +49 622154 8470; fax: +49 622154 4904.
E-mail address: j.bluemel@urz.uni-heidelberg.de (J. Blümel).

best immobilized catalysts [6,7,18], while the length of the spacer did not display a visible effect within the limited range of the alkyl chain lengths (C₁–C₄) studied. However, as it has been demonstrated by the Gladysz group, long alkyl chains can insulate a reactive moiety of a molecule, such as a long carbon rod [19a]. Furthermore, metal centers can be shielded from their surroundings by a cage of long alkyl chains [19b]. Finally, a preliminary study of the interaction of a Pt complex with a long alkyl chain between two trans-spanning phosphine ligands showed that this alkyl loop prevented the decomposition of the complex on a silica surface [20a]. Therefore, we wanted to explore the potential of monodentate and chelate linkers with very long alkyl chains (C₇ and C₁₁) as spacers, keeping in mind that the alkyl chains, due to their “brush-type” [3b] parallel arrangement, might protect catalysts bound later from any interaction with the aggressive silica surface. Furthermore, linkers with longer alkyl chains should allow enhanced mobility of metal complexes bound at their end [11b], and thus mimic homogeneous catalysis better. Finally, the mobility of the linkers is also increased by their density on the surface [11b], which is why we sought to increase the number of linkers per surface binding site.

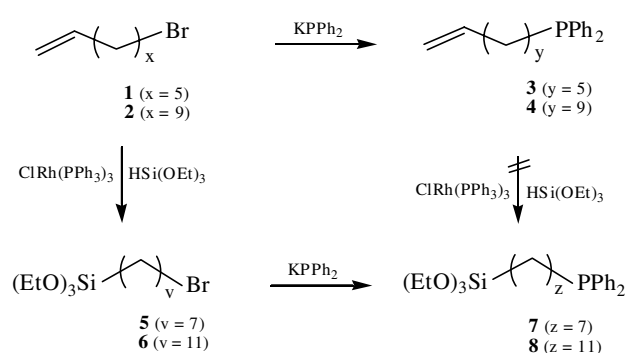
This quest can ideally be combined with the chelate concept, when two long alkyl chains with phosphine functions at their end are bound to one diethoxysilane group. The strategy here is not so much to create an exact molecular (chelate phosphine)/(metal fragment), but to provide a dense “lawn” of phosphine moieties on the surface that keeps a metal from leaching, even if it shows migrational mobility (“surface hopping”) on the surface, such as Pd [18]. Of course, the denser the surface is packed with catalyst, the less bulk material is needed, a positive factor that might be important for future industrial applications, where “dead volume” has to be minimized.

Therefore, in this work, we will present, together with corresponding model compounds, a new class of bidentate phosphine linkers with long (C₇ and C₁₁) alkyl chains, incorporating the diethoxysilane group in the center of the backbone. These linkers, in contrast to the previous ones [12] are symmetric, which is especially desirable from an analytical point of view, and it will be demonstrated that they can be immobilized in a clean and well-defined manner.

2. Results and discussion

2.1. Syntheses of monodentate phosphine linkers

For the synthesis of the monodentate phosphine linkers with ethoxysilane groups, **7** and **8**, there are in principle two routes, as outlined in Scheme 1. Starting from the commercially available unsaturated bromides **1** and **2**, one can either perform first a hydrosilylation, leading to **5** and **6**, or by reaction with KPPH₂ transform the silanes into phosphines **7** and **8**. Alternatively, one can first synthesize the unsaturated phosphines **3** and **4** from **1** and **2** [20a,20b],



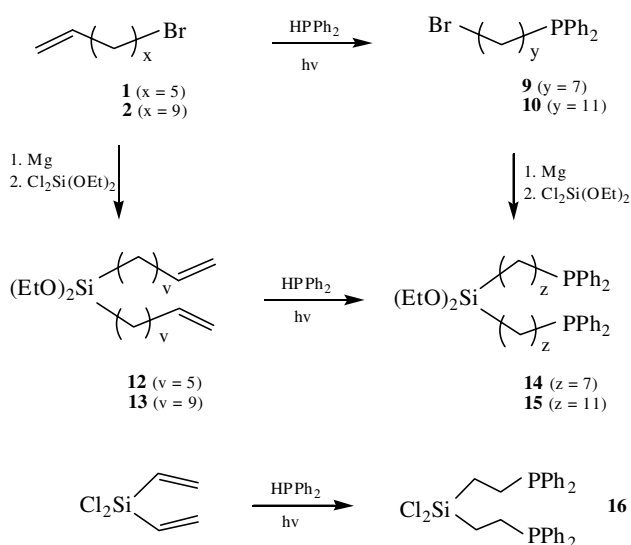
Scheme 1. Synthesis of the monodentate phosphines **7** and **8** with long alkyl chains.

and then hydrosilylate them in the final step. However, with the unprotected phosphines, we could not successfully perform the hydrosilylation catalyzed by the Wilkinson complex ClRh(PPh₃)₃, most probably because the phosphine groups of **3** and **4** coordinate to the Rh complex, thus deactivating it. Therefore, in order to avoid one more step, i.e. protecting the phosphines prior to hydrosilylation, we preferred the first route for the synthesis of **7** and **8**. Since only standard reactions are needed for the syntheses in Scheme 1, the yields are usually high. For example, **6** was obtained after purification by Kugelrohr distillation in about 70% yield, phosphine **7** in nearly 90% yield. All the compounds presented in Scheme 1 are colorless, viscous liquids. The phosphines are only moderately air sensitive in pure form, but more so in solution. The NMR signal assignments of all the compounds in this work have been done by standard 1D and 2D techniques, and by comparison with previously described linkers with Ph₂PR moieties [6a,8,11b,12,16a]. Phosphines **3** and **4** have been described earlier [20].

2.2. Syntheses of chelate phosphine linkers

One key compound for the synthesis of chelate phosphine linkers incorporating diethoxysilane groups in the center of their backbones is Cl₂Si(OEt)₂. We have optimized its synthesis starting from SiCl₄ and Me₂Si(OEt)₂, and outlined the procedure in a previous publication [8]. As presented in Scheme 2, there are in principle two synthetic routes that lead to phosphines **14** and **15**. The optimal strategy turned out to be the transformation of **1** and **2** into **12** and **13** by a Grignard reaction, and subsequently using hydrophosphination with HPPH₂ to obtain **14** and **15**. The yields along this route are high, for example **13** was available in 67% yield, **15** in 96%.

Alternatively, compounds **9** and **10** could be obtained by hydrophosphination of the corresponding bromoalkenes **1** and **2** with diphenylphosphine (Scheme 2). Then, **14** and **15** result after a Grignard reaction. The yields are very good for **10** (92%) and reasonable for **15** (75%). However, due to the formation of phosphonium salts from **9** (see below), **14** is better synthesized via route one.

Scheme 2. Synthesis of the molecular phosphines **9**, **10**, and **14–16**.

2.3. Crystal structure of **10**

Usually compounds with long alkyl chains are oily or waxy. However, in the case of phosphine **10** we succeeded to get crystals of good quality from a pentane solution at $-30\text{ }^{\circ}\text{C}$. A suitable colorless crystal was studied on a Bruker-Nonius APEX CCD diffractometer (Mo $K\alpha$ radiation, $\lambda = 0.71073\text{ \AA}$, graphite monochromator, 0.3° ω -scans) at 100 K . The intensities were corrected for Lorentz and polarization effects, an empirical absorption correction was applied using SADABS [21] based on the Laue symmetry of the reciprocal space, the structure was solved by direct methods and refined against F^2 with a full-matrix least-squares algorithm using the SHELXTL (6.12) software package [22]. Crystallographic details on data collection and structure refinement are deposited with the Cambridge Crystallographic Data Centre – CCDC No. 612526. Detailed information for data collection and structure refinement for the complex is presented in Table 1.

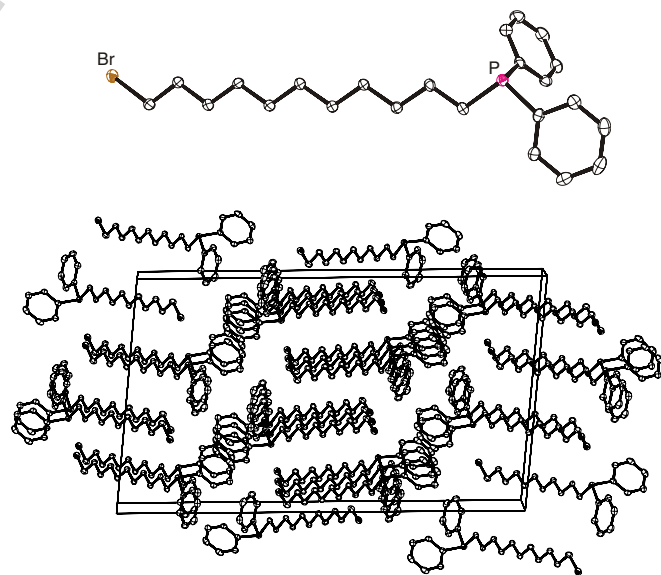
2.4. Discussion of the X-ray structure of **10**

Views of the crystal structure are shown in Fig. 1. As is clearly seen in the molecular structure (top), the $\text{Br}(\text{CH}_2)_{11}\text{P}$ chain adopts an all-anti conformation. As represented in the packing diagram (bottom), the alkyl chains are aligned parallel towards each other in stacks along the crystallographic b -axis. Parallel to the c -axis a head-to-tail arrangement took place. Hereby, the distance between the alkyl chains is always larger than the sum of the corresponding Van-der-Waals radii. A similar anti-parallel arrangement of long alkyl chains has been found in a compound by Polas et al. [24]. The tendency of longer alkyl chains to align in a parallel manner has also been described by us recently for a compound, where two alkyl chains bound to a Pt metal center by phosphine functionalities are oriented parallel to each other [20a]. Based on the crystal structure of **10**, we assume

Table 1

Crystal data and structure refinement parameters of $\text{Br}(\text{CH}_2)_{11}\text{PPh}_2$ (**10**)

Empirical formula	$\text{C}_{23}\text{H}_{32}\text{BrP}$
Formula weight	419.37
Temperature (K)	100(2)
Wavelength (\AA)	0.71073
Crystal system	monoclinic
Space group	$C2/c$
Z	8
Unit cell dimensions	
a (\AA)	18.047(2)
b (\AA)	7.5706(9)
c (\AA)	31.155(4)
β ($^{\circ}$)	95.447(2)
Volume (\AA^3)	4237.5(9)
Calculated density (g/cm^3)	1.32
Absorption coefficient (mm^{-1})	2.02
Crystal size (mm)	$0.16 \times 0.14 \times 0.04$
θ Range for data collection ($^{\circ}$)	1.3–27.9
Limiting indices	$-23 \leq h \leq 23$, $-9 \leq k \leq 9$, $-40 \leq l \leq 40$
Reflections collected	20662
Independent reflections [R_{int}]	5035 [0.051]
Observed reflections ($I > 2\sigma(I)$)	4107
Maximum and minimum transmission	0.92 and 0.74
Refinement method	full-matrix least-squares on F^2
Data/restraints/parameters	5035/0/354
Goodness-of-fit on F^2	1.13
Final R indices ($I > 2\sigma(I)$)	$R_1 = 0.053$, $wR_2 = 0.097$
Largest difference in peak and hole (e \AA^{-3})	0.75 and -0.59

Fig. 1. Crystal structure of **10** [23]. Top: molecular structure, bottom: a view of the unit cell, along the crystallographic b -axis, with the alkyl chains of **10** arranged in a parallel manner.

that the phosphine linkers bound to the silica surface will also have their alkyl chains aligned in a similar fashion, forming a “brush-type” arrangement [3b].

Compound **9** showed a striking tendency to form intra- and/or intermolecularly the phosphonium bromides that are no longer soluble in nonpolar solvents. The phosphorus

chemical shift obtained by ^{31}P CP/MAS NMR was 28.3 ppm. Together with the small chemical shift anisotropy, this is characteristic for dialkyldiphenyl phosphonium salts [16b]. The prevalence of intermolecular phosphonium bromide formation can be deduced from the mass spectrum of the material. Besides the peak for the molecular ion $[\text{M}]^+$ of **9**, fragments for $[\text{M}+\text{C}_7\text{H}_{14}]^+$, $[3\text{M}-\text{Br}]^+$, $[4\text{M}-2\text{Br}]^+$, and $[5\text{M}-2\text{Br}]^+$ are present with their characteristic isotopic distribution.

The same tendency of phosphonium formation can, albeit less pronounced, also be found for **10**. In one attempt to crystallize **10**, interestingly a single crystal of the phosphonium salt $[\text{Ph}_3\text{POH}]\text{Br}$ (**11**) could be obtained, and the crystal structure of it is in agreement with one previously reported [25]. This surprising result can, however, be easily explained at the first sight. The phosphonium salt **11** is generated via the initial formation of the dialkyldiphenyl phosphonium bromide, as proved for **9**. These bromides undergo a scrambling of the substituents at the phosphonium center, resulting in the trialkylmonoaryl, and the monoalkyltriphenyl phosphonium salts. The latter is then hydrolyzed by traces of water, liberating the alkyl substituent as the alkane, and replacing it by the OH group.

Due to the overlapping of resonances, not all, but the majority of the NMR signals of the compounds with long alkyl chains can be assigned by standard 1D and 2D NMR techniques, including $^{13}\text{C}\{^{31}\text{P}\}$ spectra. As an example, Fig. 2 shows the aliphatic region of the ^{13}C , ^1H COSY spectrum of **14**. Besides the signal of the methyl group, the seven signals for the alkyl chains are clearly visible, and they can all be assigned with the help of the ^{31}P , ^{13}C couplings.

Compound **16** was prepared as a model compound of the same type as **14** and **15**, but with shorter alkyl chain length for later studies on catalysis. Using Michler's ketone

for improving the quantum yield, **16** could easily be obtained in 58% unoptimized yield starting from the commercially available $\text{Cl}_2\text{Si}(\text{CH}=\text{CH}_2)_2$ by UV irradiation and subsequent Kugelrohr distillation. The chemical shifts and coupling constants are in excellent accord with those of the similar substances $\text{Ph}_2\text{P}(\text{CH}_2)_2\text{SiMeCl}_2$ [26a] and $\text{HSiMe}[(\text{CH}_2)_2\text{PPh}_2]_2$ [26b]. Although in the case of **16**, in contrast to the analog $(\text{EtO})_2\text{Si}(\text{CH}_2\text{PPh}_2)_2$ described earlier [8], the number of methylene groups, together with the additional Cl_2Si segment, between the phosphorus nuclei prevent “virtual couplings” [27], the ^1H NMR spectra show complicated signal patterns because the methylene protons are diastereotopic, as in the analogs given above [26].

2.5. Immobilization of the phosphine linkers

All the monodentate and chelate linkers **7**, **8**, and **14–16** can be immobilized on silica in a clean and well-defined manner, giving **7i**, **8i**, and **14i–16i** (Scheme 3). The surface coverages are in the typical range [6–8,11–14], for example 136 mg (0.26 mmol) of **16** are immobilized on 1 g of silica. The ^{31}P CP/MAS spectra show no signs of ligand destruction [11c], phosphine oxide [16a] or phosphonium salts [16b], which often occur as side products in the cases of other linkers. Furthermore, they are strongly bound in a covalent manner, and after thorough washing do not show leaching from the support. As we have demonstrated earlier, even one covalent siloxane bond between linker and support suffices for strong and irreversible binding of the linkers [11b,13]. Therefore, the linkers with the central diethoxysilane group are bound as strong as those with triethoxysilane anchoring functionalities. Fig. 3, for example,

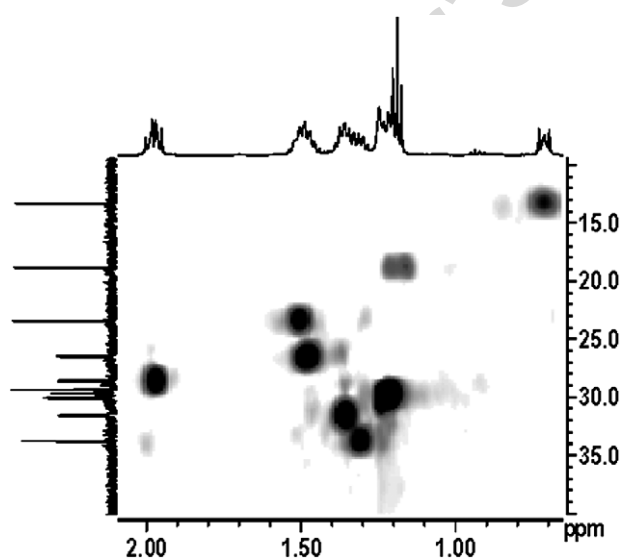
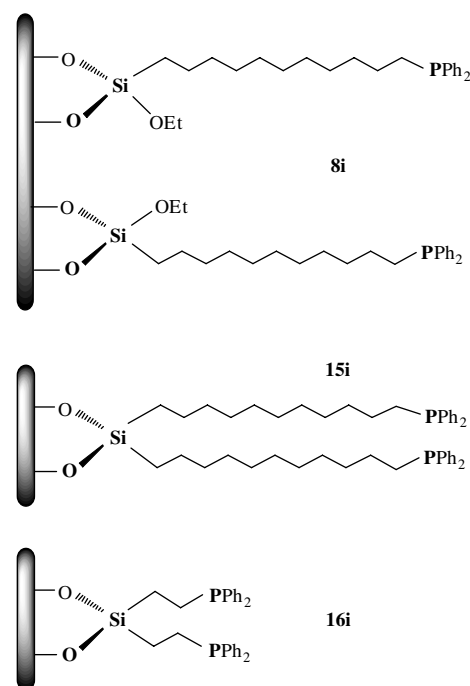


Fig. 2. ^{13}C , ^1H COSY NMR spectrum of **14** in C_6D_6 , aliphatic region only.



Scheme 3. The immobilized linkers **8i**, **15i**, and **16i**.

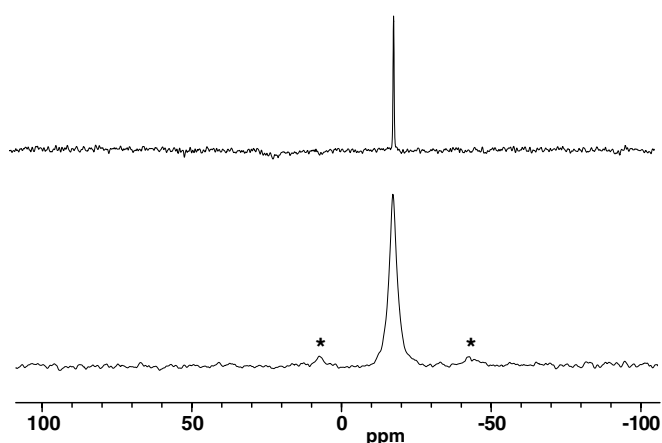


Fig. 3. ^{31}P CP/MAS (bottom, 4 kHz) and ^{31}P suspension HRMAS (top, 2 kHz, in acetone- d_6 as the suspension medium) spectra of **15i** on silica. Asterisks denote rotational sidebands. For details of the measurements, see Refs. [10,11c].

shows the ^{31}P CP/MAS spectrum of **15i** on silica at 4 kHz rotational speed (bottom spectrum). The halfwidth of the CP/MAS signal is about 470 Hz. The suspension HRMAS spectrum of **15i** in acetone gives a much narrower line with a halfwidth of merely 65 Hz even at a low spinning frequency of 2 kHz (Fig. 3, top spectrum), a tendency corresponding to earlier results [8,11c,11d,18]. This scenario also resembles the one found for monodentate linkers [11b], and it shows that the alkyl chains of the chelate versions of the linkers are as mobile as the less densely packed chains of the monodentate linkers. Taking into account the earlier studies with stationary samples measured in suspension without MAS [11b], the dense packing of the alkyl chains in the immobilized chelate linkers **14i** and **15i** should lead to even increased mobility, because any surface adsorption of the phosphine moieties is less likely, and the brush-type [3b] upright arrangement of the linkers with parallel alkyl chains prevails. The denser packing of the surface with alkyl chains in the cases of **14i–16i** as compared to **7i** and **8i** can also be deduced from their surface coverages. For example, 23 molecules of **8** and 17 molecules of chelate **15** can be bound on 100 nm² of the silica surface. Taking into account that **15** has double the number of alkyl chains per molecule as compared to monodentate **8**, the actual number of phosphine moieties per 100 nm² of silica is 34 for **15i**. So, this chelate phosphine affords about 1.5 times the number of phosphine groups per surface unit, as compared to the monodentate analog. In other words, the chelate linkers **14–16** are more surface economic with respect to binding sites on the silica surface than monodentate analogs.

In order to prove the clean and uniform binding of **14i–16i** to the support, we recorded the ^{29}Si CP/MAS spectra. As it can be seen for example in Fig. 4, besides signals for the Si nuclei in the bulk of the silica, there is a signal at -20 ppm. This chemical shift is characteristic for silanes with two alkyl groups and two siloxane bonds to the support [8]. Therefore, we conclude that although the chloro-

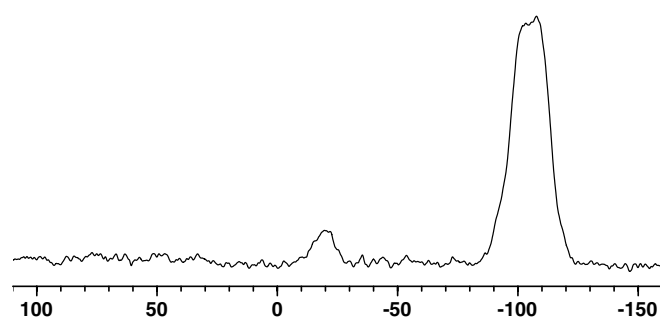


Fig. 4. ^{29}Si CP/MAS spectrum of **16i**. The details of the measurement have been described earlier [11b].

or ethoxysilane functionalities are in the middle of a long alkyl chain, they find their way to the surface and bind to it in a clean and well-defined manner. As in the case of the triethoxysilane functions in the monodentate linkers **7** and **8**, bonding via two siloxane bridges is the preferred mode [9g,11b,14].

Having demonstrated that all the linkers described in this work can be immobilized without any problems, we conclude that they are ready now to be applied as metal scavengers, or as linkers for immobilized catalysts.

3. Conclusion

New monodentate and chelate linkers with long alkyl chains for immobilization of metal complexes on oxide supports have been described and fully characterized. Their “brush-type” arrangement on the surface has been made plausible by an X-ray determination, as well as by ^{31}P CP/MAS and HRMAS NMR. Due to this parallel and dense arrangement of the alkyl chains, especially the chelate ligands should later protect immobilized metal complexes from any contact with the aggressive silica surface, thus preventing their premature deactivation and leading to recyclable catalysts with longer lifetimes. This option will be explored in our future work.

4. Experimental

All reactions were carried out in Schlenk flasks under purified nitrogen. The solvents were dried and distilled according to standard procedures prior to use. Support material: Silica gel 40 (Merck, specific surface area 750 m²/g, average pore diameter 40 Å, particle size 0.063–0.2 mm). The solution NMR spectra were recorded on routine Bruker spectrometers at field strengths corresponding to 250, 300, and 500 MHz. The solid-state NMR spectra were recorded on a fully digital Bruker Avance 400 NMR spectrometer equipped with a 4 mm MAS probehead. This probehead was used for both classical and suspension MAS measurements. For CP/MAS parameters see Ref. [10], for suspension HRMAS measurement conditions see Ref. [11c]. The signal assignments are based on comparisons with previous phosphine linkers [6a,12], ^{31}P -decoupled, and two-dimensional correlation spectra.

4.1. (EtO)₃Si(CH₂)₇Br (5)

1.105 g (6.24 mmol) of CH₂=CH(CH₂)₅Br, together with a catalytic amount of ClRh(PPh₃)₃, and 1.040 g (6.33 mmol) of (EtO)₃SiH were dissolved in 10 ml of toluene and refluxed at 85 °C for 16 h. After removal of the toluene in vacuo, the product was purified by Kugelrohr distillation (110 °C, 0.15 mbar). Compound **5** was obtained as a colorless, viscous liquid in 71.8% yield (1.53 g, 4.48 mmol). ¹H NMR (C₆D₆, 300.1 MHz): δ 3.81 (q, 6H, ³J(H,H) = 7.0 Hz, CH₂O), 2.94 (t, 2H, ³J(H,H) = 6.9 Hz, CH₂Br), 1.58–1.43 (m, br, 4H, overlapping SiCH₂CH₂ and CH₂CH₂Br), 1.29–1.06 (m, 6H, overlapping CH₂CH₂CH₂(CH₂)₂Br), 1.18 (t, 9H, ³J(H,H) = 7.0 Hz, CH₃), 0.71 (t, 2H, ³J(H,H) = 8.3 Hz, SiCH₂). ¹³C NMR (C₆D₆, 75.5 MHz): δ 58.47 (CH₂O), 33.65 (CH₂Br), 33.18* (CH₂CH₂Br), 33.06 (Si(CH₂)₂CH₂), 28.68° (CH₂(CH₂)₂Br), 28.26° (CH₂(CH₂)₃Br), 23.29 (SiCH₂CH₂), 18.64 (CH₃), 11.12 (SiCH₂). *°assignments interchangeable. MS (FD⁺) *m/z* (%): 340.1 (M⁺, 91), 297.1 ([M–OEt]⁺, 100), 163.1 ([M–(CH₂)₇Br]⁺, 85). EA Calc. C, 45.74; H, 8.56. Found: C, 45.82; H, 8.61%.

4.2. (EtO)₃Si(CH₂)₁₁Br (6)

1.923 g (8.25 mmol) of CH₂=CH(CH₂)₇Br, together with a catalytic amount of ClRh(PPh₃)₃, and 1.354 g (8.24 mmol) of (EtO)₃SiH were dissolved in 15 ml of toluene and refluxed at 90 °C for 16 h. After removal of all volatile matter in vacuo, the product was purified by Kugelrohr distillation (130 °C, 0.15 mbar). Compound **6** was obtained as a colorless, viscous liquid in 69.3% yield (2.27 g, 5.71 mmol). ¹H NMR (CDCl₃, 500.1 MHz): δ 3.80 (q, 6H, ³J(H,H) = 6.9 Hz, CH₂O), 2.38 (t, 2H, ³J(H,H) = 6.9 Hz, CH₂Br), 1.83 (qui, 2H, ³J(H,H) = 7.8 Hz, CH₂CH₂Br), 1.38 (m, 4H, overlapping SiCH₂CH₂ and CH₂(CH₂)₂Br), 1.32–1.23 (m, br, 12H, overlapping Si(CH₂)₂CH₂CH₂CH₂CH₂CH₂CH₂), 1.21 (t, 9H, ³J(H,H) = 6.9 Hz, CH₃), 0.61 (t, 2H, ³J(H,H) = 8.4 Hz, SiCH₂). ¹³C NMR (CDCl₃, 125.8 MHz): δ 58.23 (CH₂O), 33.94 (CH₂Br), 33.13 (Si(CH₂)₂CH₂), 32.81 (CH₂CH₂Br), 29.50* (Si(CH₂)₃CH₂), 29.44* (Si(CH₂)₄CH₂), 29.39* (Si(CH₂)₅CH₂), 29.19* (Si(CH₂)₆CH₂), 28.73 (CH₂(CH₂)₃Br), 28.14 (CH₂(CH₂)₂Br), 23.51 (SiCH₂CH₂), 18.26 (CH₃), 10.35 (SiCH₂). *assignments interchangeable. MS (FAB⁺) *m/z* (%): 397.4 ([M]⁺, 50), 316.3 ([M–Br]⁺, 13), 163.1 ([M–(CH₂)₁₁Br]⁺, 100). HR-MS (FAB) *m/z* (%): 397.1735 ([M]⁺, 100), calc. 397.1773. EA Calc. C, 51.37; H, 9.38. Found: C, 51.40; H, 9.52%.

4.3. (EtO)₃Si(CH₂)₇PPh₂ (7)

755 mg (2.21 mmol) of (EtO)₃Si(CH₂)₇Br (**5**) was dissolved in 15 ml of pentane and cooled to –10 °C. Then 4.5 ml of a 0.5 M solution of KPPH₂ (504 mg, 2.25 mmol) in THF was added dropwise over 2 h. After stirring for 1 h at ambient temperature, the precipitated salts were filtered

off, and the solvents were removed in vacuo. Compound **7** was obtained as a colorless, viscous liquid in 79.0% yield (780 mg, 1.75 mmol). ¹H NMR (C₆D₆, 500.1 MHz): δ 7.47–7.41 (m, 4H, H_o), 7.12–7.04 (m, 6H, overlapping H_m, H_p), 3.81 (q, 6H, ³J(H,H) = 7.0 Hz, CH₂O), 1.95 (t, 2H, ³J(H,H) = 7.9 Hz, CH₂P), 1.54 (m, 2H, SiCH₂CH₂), 1.45 (m, 2H, CH₂CH₂P), 1.38–1.26 (m, broad, 4H, overlapping Si(CH₂)₂CH₂ and CH₂(CH₂)₂P), 1.21–1.15 (m, br, 2H, overlapping Si(CH₂)₃CH₂ and CH₂CH₂P), 1.18 (t, 9H, ³J(H,H) = 7.0 Hz, CH₃), 0.71 (t, 2H, ³J(H,H) = 8.2 Hz, SiCH₂). ¹³C NMR (C₆D₆, 125.8 MHz): δ 140.06 (d, ¹J(P,C) = 14.8 Hz, C_i), 133.14 (d, ²J(P,C) = 18.6 Hz, C_o), 128.57 (s, C_p), 128.56 (d, ³J(P,C) = 9.8 Hz, C_m), 58.31 (CH₂O), 33.44 (Si(CH₂)₂CH₂), 31.52 (d, ³J(P,C) = 12.7 Hz, CH₂(CH₂)₂P), 29.34 (CH₂(CH₂)₃P), 28.59 (d, ¹J(P,C) = 12.5 Hz, CH₂P), 26.46 (d, ²J(P,C) = 16.4 Hz, CH₂CH₂P), 23.38 (SiCH₂CH₂), 18.65 (CH₃), 11.16 (SiCH₂). ³¹P NMR (C₆D₆, 121.5 MHz): δ –16.23*. ²⁹Si NMR (C₆D₆, 99.4 MHz): δ –44.8. MS (FAB⁺) *m/z* (%): 447.5 ([M+H]⁺, 100), 417.4 ([M–Et]⁺, 28), 186.1 ([M–(CH₂)₇Si(OEt)₃]⁺, 31). HR-MS (FAB) *m/z* (%): 447.2457 ([M+H]⁺, 100), calc. 447.2484. EA Calc. C, 67.23; H, 8.80; P, 6.93. Found: C, 67.62; H, 8.58; P, 7.54%. ³¹P CP/MAS of **7i**: δ –17.1. Surface coverage of **7i**: 28 molecules of **7** on 100 nm² of silica.

4.4. (EtO)₃Si(CH₂)₁₁PPh₂ (8)

910 mg (2.29 mmol) of (EtO)₃Si(CH₂)₁₁Br (**6**) was dissolved in 20 ml of pentane and cooled to –10 °C. Then 4.6 ml of a 0.5 M solution of KPPH₂ (515 mg, 2.30 mmol) in THF was added dropwise over 2 h. After stirring for one more hour at ambient temperature, the precipitated salts were filtered off, and the solvents were removed in vacuo. Compound **8** was obtained as a colorless, viscous liquid in 89.4% yield (1.029 g, 2.05 mmol). ¹H NMR (C₆D₆, 300.1 MHz): δ 7.48–7.42 (m, 4H, H_o), 7.12–6.99 (m, 6H, overlapping H_m, H_p), 3.82 (q, 6H, ³J(H,H) = 6.9 Hz, CH₂O), 1.97 (t, 2H, ³J(H,H) = 8.2 Hz, CH₂P), 1.64 (qui, 2H, ³J(H,H) = 7.9 Hz, SiCH₂CH₂), 1.54–1.10 (m, 16H, overlapping (CH₂)₈CH₂P), 1.19 (t, 9H, ³J(H,H) = 6.9 Hz, CH₃), 0.77 (t, 2H, ³J(H,H) = 8.3 Hz, SiCH₂). ¹³C NMR (C₆D₆, 125.8 MHz): δ 140.07 (d, ¹J(P,C) = 14.7 Hz, C_i), 133.14 (d, ²J(P,C) = 18.6 Hz, C_o), 128.70 (s, C_p), 128.60 (d, ³J(P,C) = 6.4 Hz, C_m), 58.44 (CH₂O), 33.60 (Si(CH₂)₂CH₂), 31.59 (d, ³J(P,C) = 12.4 Hz, CH₂(CH₂)₂P), 30.06* (CH₂(CH₂)₃P), 29.97* (CH₂(CH₂)₄P), 29.92* (CH₂(CH₂)₅P), 29.80* (CH₂(CH₂)₆P), 29.67 (CH₂(CH₂)₇P), 28.65 (d, ¹J(P,C) = 12.6 Hz, CH₂P), 26.46 (d, ²J(P,C) = 16.4 Hz, CH₂CH₂P), 23.48 (SiCH₂CH₂), 18.62 (CH₃), 11.22 (SiCH₂). *Interchangeable assignments. ³¹P NMR (C₆D₆, 121.5 MHz): δ –16.30. MS (FAB⁺) *m/z* (%): 503.5 ([M+H]⁺, 100), 199.2 ([M–(CH₂)₉Si(OEt)₃]⁺, 98), 185.1 ([M–(CH₂)₁₀Si(OEt)₃]⁺, 61). HR-MS (FAB) *m/z* (%): 503.3080 ([M+H]⁺, 100), calc. 503.3110. EA Calc. C, 69.28; H, 9.42. Found: C, 70.15; H, 9.43%. ³¹P CP/MAS of **8i**: δ –17.2. Surface coverage of **8i**: 23 molecules of **8** on 100 nm² of silica.

4.5. $Br(CH_2)_7PPh_2$ (**9**)

400 mg (1.6 mmol) of **1**, together with 430 mg (3.30 mmol) of HPPH₂, was placed into a UV reactor and irradiated for 48 h at ambient temperature while stirring vigorously. After removal of all volatile material, compound **9** was obtained as a colorless, microcrystalline powder in less than 1% yield, due to the formation of phosphonium salts (see text). ¹H NMR (C₆D₆, 300.1 MHz): δ 7.50–7.40 (m, 4H, H_o), 7.10–7.00 (m, 6H, overlapping H_m, H_p), 2.91 (t, 2H, ³J(H,H) = 6.8 Hz, BrCH₂), 1.92 (t, 2H, ³J(H,H) = 7.5 Hz, CH₂P), 1.40 (m, 2H, BrCH₂CH₂), 1.39 (m, 2H, CH₂CH₂P), 1.12 (Br(CH₂)₄CH₂), 1.02 (m, 2H, Br(CH₂)₂-CH₂), 0.81 (m, 2H, Br(CH₂)₃CH₂). ¹³C NMR (C₆D₆, 75.5 MHz): δ 139.92 (d, ¹J(P,C) = 14.9 Hz, C_i), 133.11 (d, ²J(P,C) = 18.6 Hz, C_o), 128.79 (s, C_p), 128.77 (d, ³J(P,C) = 16.5 Hz, C_m), 33.57 (BrCH₂), 32.95 (BrCH₂CH₂), 31.17 (d, ³J(P,C) = 12.5 Hz, CH₂(CH₂)₂P), 28.54 (Br(CH₂)₃CH₂), 28.50 (d, ¹J(P,C) = 12.4 Hz, CH₂P), 28.16 (Br(CH₂)₂CH₂), 26.28 (d, ²J(P,C) = 16.5 Hz, CH₂CH₂P). ³¹P NMR (C₆D₆, 121.5 MHz): δ -16.52. MS (FAB⁺) *m/z* (%): 363.3 (M⁺, 65).

4.6. $Br(CH_2)_{11}PPh_2$ (**10**)

3.270 g (14.02 mmol) of **2**, together with 2.620 g (14.07 mmol) of HPPH₂, was placed into a UV reactor and irradiated for 4 h at ambient temperature while stirring vigorously. Then the reaction mixture was dissolved in pentane and recrystallized at -25 °C. Compound **10** was obtained as a colorless, microcrystalline powder in 92.0% yield (5.430 g, 12.94 mmol). ¹H NMR (toluene-*d*₈, 500.1 MHz): δ 7.46–7.42 (m, 4H, H_o), 7.13–7.07 (m, 6H, overlapping H_m, H_p), 2.99 (t, 2H, ³J(H,H) = 6.9 Hz, BrCH₂), 1.99 (t, 2H, ³J(H,H) = 6.9 Hz, CH₂P), 1.54 (qui, 2H, ³J(H,H) = 7.2 Hz, BrCH₂CH₂), 1.48 (m, 2H, CH₂CH₂P), 1.40 (m, 2H, CH₂(CH₂)₂P), 1.25–1.05 (m, 12H, overlapping Br(CH₂)₂(CH₂)₆). ¹³C NMR (toluene-*d*₈, 125.8 MHz): δ 140.67 (d, ¹J(P,C) = 14.9 Hz, C_i), 133.73 (d, ²J(P,C) = 18.6 Hz, C_o), 129.78 (s, C_p), 129.19 (d, ³J(P,C) = 4.2 Hz, C_m), 34.05 (BrCH₂), 33.79 (Br(CH₂)-CH₂), 32.30 (d, ³J(P,C) = 12.6 Hz, CH₂(CH₂)₂P), 30.60 (overlapping CH₂(CH₂)₄P and CH₂(CH₂)₅P), 30.50* (Br(CH₂)₃CH₂), 30.41* (Br(CH₂)₄CH₂), 29.80* (CH₂-(CH₂)₃P), 29.32 (d, ¹J(P,C) = 12.8 Hz, CH₂P), 29.13 (Br(CH₂)₂CH₂), 27.16 (d, ²J(P,C) = 16.3 Hz, CH₂CH₂P). *Interchangeable assignments. ³¹P NMR (toluene-*d*₈, 202.47 MHz): δ -16.64. MS (FAB⁺) *m/z* (%): 435.3 ([M+O]⁺, 100), 419.3 (M⁺, 42). HR-MS (FAB) *m/z* (%): 435.1432 ([M+O+H]⁺, 100), calc. 435.1452.

4.7. $(EtO)_2Si[(CH_2)_5CH=CH_2]_2$ (**12**)

500 mg (2.64 mmol) of Cl₂Si(OEt)₂ was combined with 210 mg (8.64 mmol) Mg powder and 10 ml ether. Then 1.284 g (7.25 mmol) of **1**, dissolved in 10 ml of ether, was added dropwise while stirring vigorously. Subsequently the reaction mixture was stirred for 1 h at 35 °C, and for

one more hour at ambient temperature. After removal of all volatile matter in vacuo the residue was extracted with pentane and precipitated salts were filtered off. Compound **12** was obtained as a colorless oil with a yield of 39.0% (322 mg, 1.03 mmol) with respect to Cl₂Si(OEt)₂ after removal of the solvent in vacuo. ¹H NMR (C₆D₆, 500.1 MHz): δ 5.78 (m, 2H, CH), 5.00 (m, 4H, =CH₂), 3.72 (q, 4H, ³J(H,H) = 7.0 Hz, CH₂O), 1.98 (m, 4H, =CHCH₂), 1.49 (m, 4H, SiCH₂CH₂), 1.34 (m, 8H, overlapping Si(CH₂)₂(CH₂)₂), 1.19 (t, 6H, ³J(H,H) = 7.0 Hz, CH₃), 0.69 (t, 4H, ³J(H,H) = 9.7 Hz, SiCH₂). ¹³C NMR (C₆D₆, 125.8 MHz): δ 139.19 (=CH-), 114.48 (=CH₂), 58.19 (CH₂O), 34.15 (=CHCH₂), 33.26* (Si(CH₂)₂CH₂), 29.00* (Si(CH₂)₃CH₂), 23.26 (SiCH₂CH₂), 18.78 (CH₃), 13.17 (SiCH₂). *Interchangeable assignments. ²⁹Si NMR (C₆D₆, 99.4 MHz): δ -7.39. MS (EI) *m/z* (%): 267 ([M-OEt]⁺, 37), EA Calc. C, 69.17; H, 11.61. Found: C, 69.42; H, 11.56%.

4.8. $(EtO)_2Si[(CH_2)_9CH=CH_2]_2$ (**13**)

To 493 mg (20.28 mmol) of Mg powder, a solution of 4.77 g (20.45 mmol) **2** in 20 ml of ether was added dropwise within 2 h. After heating up the mixture to the boiling point, the mixture was stirred at 30 °C for 16 h, during which time the Mg was consumed, and the color changed from white to light grey. In a second Schlenk flask, 1.930 g (10.21 mmol) of Cl₂Si(OEt)₂ was dissolved in 10 ml of ether and cooled to 0 °C. Within 1 h the Grignard mixture was added dropwise. After 2 h of stirring at ambient temperature the precipitated salts were filtered off, and the solvent was removed in vacuo. Compound **13** was obtained as a colorless, viscous liquid in 67.3% yield (2.920 g, 6.87 mmol) after Kugelrohr distillation (171 °C, 0.35 mbar). ¹H NMR (C₆D₆, 500.1 MHz): δ 5.40 (m, 2H, =CH), 5.02 (m, 4H, =CH₂), 3.76 (q, 4H, ³J(H,H) = 6.9 Hz, CH₂O), 1.99 (m, 8H, overlapping =CHCH₂CH₂), 1.59 (qui, 4H, ³J(H,H) = 8.0 Hz, SiCH₂CH₂), 1.42 (qui, 4H, ³J(H,H) = 7.4 Hz, CH₂(CH₂)₂Si), 1.34–1.23 (m, 16H, overlapping Si(CH₂)₃(CH₂)₄), 1.20 (t, 6H, ³J(H,H) = 6.9 Hz, CH₃), 0.78 (t, 4H, ³J(H,H) = 8.3 Hz, SiCH₂). ¹³C NMR (C₆D₆, 125.8 MHz): δ 139.24 (=CH-), 114.49 (=CH₂), 58.24 (CH₂O), 34.22 (two overlapping signals, =CHCH₂CH₂), 33.92 (Si(CH₂)₂CH₂), 30.18* (Si(CH₂)₃-CH₂), 30.10* (Si(CH₂)₄CH₂), 29.95* (Si(CH₂)₅CH₂), 29.36* (Si(CH₂)₆CH₂), 23.52 (SiCH₂CH₂), 18.82 (CH₃), 13.34 (SiCH₂). *Interchangeable assignments. MS (FAB⁺) *m/z* (%): 425.6 ([M]⁺, 20), 335.5 ([M-(OEt)₂]⁺, 4), 271.4 ([M-CH₂=CH(CH₂)₉]⁺, 41), 227.4 ([M-CH₂=CH-(CH₂)₉-EtO]⁺, 100). HR-MS (FAB) *m/z* (%): 425.3798 ([M+H]⁺, 100), calc. 425.3814.

4.9. $(EtO)_2Si[(CH_2)_7PPh_2]_2$ (**14**)

126 mg (0.40 mmol) of (EtO)₂Si[(CH₂)₅CH=CH₂]₂ (**12**) was combined with 150 mg (0.81 mmol) of HPPH₂, and irradiated with a UV lamp for 48 h at ambient temperature.

Compound **14** was obtained as a colorless powder in 92.3% yield (253 mg, 0.37 mmol). ^1H NMR (C_6D_6 , 300.1 MHz): δ 7.45 (m, 8H, H_o), 7.10–7.00 (m, 12H, overlapping H_m , H_p), 3.76 (q, 4H, $^3J(\text{H,H}) = 6.9$ Hz, CH_2O), 1.96 (m, 4H, CH_2P), 1.50 (m, 4H, SiCH_2CH_2), 1.45 (m, 4H, $\text{CH}_2\text{CH}_2\text{P}$), 1.38 (m, 4H, $\text{CH}_2(\text{CH}_2)_2\text{P}$), 1.31 (m, 4H, $\text{Si}(\text{CH}_2)_2\text{CH}_2$), 1.22 (m, 4H, $\text{Si}(\text{CH}_2)_3\text{CH}_2$), 1.18 (t, 6H, $^3J(\text{H,H}) = 6.9$ Hz, CH_3), 0.71 (t, 2H, $^3J(\text{H,H}) = 8.2$ Hz, SiCH_2). ^{13}C NMR (C_6D_6 , 75.5 MHz): δ 140.04 (d, $^1J(\text{P,C}) = 14.8$ Hz, C_i), 133.13 (d, $^2J(\text{P,C}) = 18.5$ Hz, C_o), 128.79 (s, C_p), 128.56 (d, $^3J(\text{P,C}) = 9.8$ Hz, C_m), 61.57 (CH_2O), 33.75 ($\text{Si}(\text{CH}_2)_2\text{CH}_2$), 31.56 (d, $^3J(\text{P,C}) = 12.7$ Hz, $\text{CH}_2(\text{CH}_2)_2\text{P}$), 29.37 ($\text{CH}_2(\text{CH}_2)_3\text{P}$), 28.60 (d, $^1J(\text{P,C}) = 12.5$ Hz, CH_2P), 26.48 (d, $^2J(\text{P,C}) = 16.3$ Hz, $\text{CH}_2\text{CH}_2\text{P}$), 23.41 (SiCH_2CH_2), 18.80 (CH_3), 13.29 (SiCH_2). ^{31}P NMR (C_6D_6 , 121.5 MHz): δ -16.60. MS (FAB^+) m/z (%): 685.6 ($[\text{M}+\text{H}]^+$, 28). HR-MS (FAB^+) m/z (%): 685.3766 ($[\text{M}+\text{H}]^+$, 100), calc. 685.3759. ^{31}P CP/MAS of **7i**: δ -16.9. Surface coverage of **14i**: about 19 molecules of **14** on 100 nm^2 of silica.

4.10. $(\text{EtO})_2\text{Si}[(\text{CH}_2)_{11}\text{PPh}_2]_2$ (**15**)

4.10.1. Synthesis route 1

255 mg (0.60 mmol) of **13** was combined with 224 mg (1.20 mmol) of HPPH_2 and irradiated for 4 h at ambient temperature in a UV reactor while stirring vigorously. The excess of unreacted HPPH_2 was removed by Kugelrohr distillation, and 460 mg (0.58 mmol) of compound **15** was obtained as a colorless, viscous liquid, corresponding to a yield of 96.2%.

4.10.2. Synthesis route 2

20 mg of Mg powder (0.82 mmol) was combined with a solution of 347 mg (0.83 mmol) of **10** in 20 ml of ether. The reaction mixture was refluxed for 4 h with a bath temperature of 45°C , during which time the mixture turned from white to light grey. In a different Schlenk flask, 80 mg (0.40 mmol) of $\text{Cl}_2\text{Si}(\text{OEt})_2$ were dissolved in 20 ml of ether. To this reaction vessel, in the course of 2 h, the Grignard reagent was added dropwise while stirring vigorously. The reaction mixture was stirred for 12 h at ambient temperature. The bromide salts were removed from the white suspension by filtration. After removal of the solvent, 247 mg (0.31 mmol) of **15** was obtained as a colorless, viscous oil, corresponding to a yield of 74.9%. ^1H NMR (C_6D_6 , 250.3 MHz): δ 7.45 (m, 8H, H_o), 7.12–7.01 (m, 12H, overlapping H_m , H_p), 3.76 (q, 4H, $^3J(\text{H,H}) = 6.9$ Hz, CH_2O), 1.98 (t, 4H, $^3J(\text{H,H}) = 7.6$ Hz, CH_2P), 1.62 (m, 4H, PCH_2CH_2), 1.54–1.21 (m, broad, 16H, overlapping $(\text{CH}_2)_8\text{CH}_2\text{Si}$), 1.19 (t, 6H, $^3J(\text{H,H}) = 6.9$ Hz, CH_3), 0.78 (t, 4H, $^3J(\text{H,H}) = 8.3$ Hz, SiCH_2). ^{13}C NMR (C_6D_6 , 75.5 MHz): δ 139.99 (d, $^1J(\text{P,C}) = 14.8$ Hz, C_i), 133.06 (d, $^2J(\text{P,C}) = 18.5$ Hz, C_o), 128.57 (d, $^3J(\text{P,C}) = 6.5$ Hz, C_m), 128.50 (s, C_p), 58.37 (CH_2O), 33.52 ($\text{Si}(\text{CH}_2)_2\text{CH}_2$), 31.50

(d, $^3J(\text{P,C}) = 12.4$ Hz, $\text{CH}_2(\text{CH}_2)_2\text{P}$), 29.97* ($\text{CH}_2(\text{CH}_2)_3\text{P}$), 29.91* ($\text{CH}_2(\text{CH}_2)_4\text{P}$), 29.84* ($\text{CH}_2(\text{CH}_2)_5\text{P}$), 29.71* ($\text{CH}_2(\text{CH}_2)_6\text{P}$), 29.59* ($\text{CH}_2(\text{CH}_2)_7\text{P}$), 28.57 (d, $^1J(\text{P,C}) = 12.5$ Hz, CH_2P), 26.39 (d, $^2J(\text{P,C}) = 16.4$ Hz, $\text{CH}_2\text{CH}_2\text{P}$), 23.39 (SiCH_2CH_2), 18.55 (CH_3), 11.13 (SiCH_2). *Interchangeable assignments. ^{31}P NMR (C_6D_6 , 101.3 MHz): δ -16.31. MS (FAB^+) m/z (%): 797 ($[\text{M}]^+$, 3), 339 ($[\text{M}-(\text{CH}_2)_{11}\text{PPh}_2]^+$, 32), 199.2 ($[\text{Ph}_2\text{PCH}_3]^+$, 100), 185.2 ($[\text{PPh}_2]^+$, 75). HR-MS (FAB) m/z (%): 797.5012 ($[\text{M}+\text{H}]^+$, 55), calc. 797.5011. ^{31}P CP/MAS of **15i**: δ -17.2. Surface coverage of **15i**: about 17 molecules of **15** on 100 nm^2 of silica.

4.11. $\text{Cl}_2\text{Si}(\text{CH}_2\text{CH}_2\text{PPh}_2)_2$ (**16**)

A mixture of $\text{Cl}_2\text{Si}(\text{CH}=\text{CH}_2)_2$ (350 mg, 2.29 mmol), 8 mg of $[(\text{CH}_3)_2\text{N}(p\text{-C}_6\text{H}_4)]_2\text{CO}$ (Michler's ketone), and HPPH_2 (1.30 g, 6.98 mmol) in 8 ml of THF was irradiated with a UV lamp for 60 h at ambient temperature. Then about 80% of the solvent was removed, and traces of solid matter were removed by extraction with 10 ml of toluene. The product was separated from unreacted volatile starting materials by Kugelrohr distillation. At 160°C and 0.8 mbar, **16** was obtained as a very viscous, colorless liquid in 58.2% yield (696 mg, 1.33 mmol). ^1H NMR (C_6D_6 , 500.1 MHz): δ 7.36 (dt, $^3J(\text{P,H}) = ^3J(\text{H,H}) = 7.9$ Hz, $^4J(\text{H}_o, \text{H}_p) = 1.5$ Hz, 8H, H_o), 7.06–7.04 (m, 12H, overlapping H_m , H_p), 2.11 (virtual t, distance between lines 8.2 Hz, 4H, PCH_2), 1.04 (virtual q, distance between outer lines 26.2 Hz, distance between inner lines: 8.2 Hz, 4H, CH_2Si). ^{13}C NMR (C_6D_6 , 125.8 MHz): δ 138.60 (d, $^1J(\text{P,C}) = 15.1$ Hz, C_i), 133.07 (d, $^2J(\text{P,C}) = 18.6$ Hz, C_o), 128.96 (s, C_p), 128.84 (d, $^3J(\text{P,C}) = 6.5$ Hz, C_m), 20.53 (d, $^1J(\text{P,C}) = 16.3$ Hz, PCH_2), 16.14 (dd, $^2J(\text{P,C}) = 14.8$ Hz, $^4J(\text{P,C}) = 1.4$ Hz, CH_2Si). ^{31}P NMR (C_6D_6 , 121.9 MHz) δ -10.81. ^{29}Si NMR (C_6D_6 , 99.4 MHz) δ 32.01 (t, $^3J(\text{P,Si}) = 28.5$ Hz). HR-MS (EI) m/z (%): 524.0833 ($[\text{M}]^+$, 40), calc. 524.0812; 339.0252 ($[\text{M}-\text{PPh}_2]^+$, 100), calc. 339.0292; 310.9951 ($[\text{M}-\text{C}_2\text{H}_4\text{PPh}_2]^+$, 31), calc. 310.9979. ^{31}P MAS of **16i**: δ -10.44 (4 kHz); ^{29}Si CP/MAS of **16i**: δ -20.4 (4 kHz). Surface coverage of **16i**: 95 mg of **16** is bound to 700 mg of silica, corresponding to about 21 particles per 100 nm^2 .

5. Supporting information

Crystallographic data for the structural analysis of **10** have been deposited with the Cambridge Crystallographic Data Centre, CCDC No. 612526 for **10**.

Copies of this information may be obtained free of charge from: The Director, CCDC, 12 Union Road, Cambridge, CB2 1EZ UK, fax: (int code) +44 1223 336 033 or email: deposit@ccdc.cam.ac.uk or www: <http://www.ccdc.cam.ac.uk>.

Acknowledgement

We thank the Deutsche Forschungsgemeinschaft (SFB 623) for financial support.

References

- [1] (a) K.C. Nicolaou, R. Hanco, W. Hartwig (Eds.), *Handbook of Combinatorial Chemistry*, vols. 1–2, Wiley-VCH, Weinheim, 2002; (b) S.R. Wilson, A.W. Czarnik (Eds.), *Combinatorial Chemistry*, John Wiley & Sons, New York, 1997; (c) W. Bannworth, E. Felder (Eds.), *Combinatorial Chemistry*, Wiley-VCH, Weinheim, 2000; (d) G. Jung, *Combinatorial Chemistry*, Wiley-VCH, Weinheim, 1999.
- [2] (a) P. Seneci, *Solid-Phase Synthesis and Combinatorial Technologies*, John Wiley & Sons, New York, 2000; (b) F. Zaragoza Dörwald, *Organic Synthesis on Solid Phase*, Wiley-VCH, Weinheim, 2000.
- [3] (a) E.F. Vansant, P. VanDer Voort, K.C. Vrancken, *Characterization and Chemical Modification of the Silica Surface*, Elsevier, Amsterdam, 1995; (b) R.P.W. Scott, *Silica Gel and Bonded Phases*, John Wiley and Sons, New York, 1993; (c) G.A. Subramanian, *Practical Approach to Chiral Separations by Liquid Chromatography*, VCH, Weinheim, 1994; (d) R.K. Iler, *The Chemistry of Silica*, John Wiley, New York, 1979.
- [4] (a) F.R. Hartley, *Supported Metal Complexes*, D. Reidel Publishing Co., Dordrecht, Holland, 1985, and literature cited therein; (b) J.H. Clark, *Supported Reagents in Organic Reactions*, VCH, Weinheim, 1994; (c) J.A. Gladysz (Ed.), *Chem. Rev.* 102 (10) (2002) (Special issue on recoverable catalysts and reagents); (d) D.E. DeVos, I.F.J. Vankelecom, P.A. Jacobs (Eds.), *Chiral Catalyst Immobilization and Recycling*, Wiley, VCH, Weinheim, 2000.
- [5] (a) For some representative examples see: H. Gao, R.J. Angelici, *Organometallics* 18 (1999) 989; (b) Z. Lu, E. Lindner, H.A. Mayer, *Chem. Rev.* 102 (2002) 3543; (c) H. Gao, R.J. Angelici, *J. Am. Chem. Soc.* 119 (1997) 6937; (d) P. McMorn, G.J. Hutchings, *Chem. Soc. Rev.* 33 (2004) 108.
- [6] (a) C. Merckle, S. Haubrich, J. Blümel, *J. Organomet. Chem.* 627 (2001) 44; (b) C. Merckle, J. Blümel, *Adv. Synth. Catal.* 345 (2003) 584; (c) C. Merckle, J. Blümel, *Top. Catal.* 34 (2005) 5.
- [7] (a) K.D. Behringer, J. Blümel, *Inorg. Chem.* 35 (1996) 1814; (b) S. Reinhard, P. Soba, F. Rominger, J. Blümel, *Adv. Synth. Catal.* 345 (2003) 589; (c) S. Reinhard, K.D. Behringer, J. Blümel, *New J. Chem.* 27 (2003) 776.
- [8] M. Bogza, T. Oeser, J. Blümel, *J. Organomet. Chem.* 690 (2005) 3383.
- [9] (a) A.T. Bell, A. Pines (Eds.), *NMR Techniques in Catalysis*, Marcel Dekker, Inc., New York, 1994; (b) G. Engelhardt, D. Michel, *High-Resolution Solid-State NMR of Silicates and Zeolites*, John Wiley & Sons, New York, 1987; (c) C.A. Fyfe, *Solid-State NMR for Chemists*, C.F.C. Press, Guelph, Canada, 1983; (d) E.O. Stejskal, J.D. Memory, *High Resolution NMR in the Solid State*, Oxford University Press, New York, 1994; (e) J.J. Fitzgerald (Ed.), *Solid-State NMR Spectroscopy of Inorganic Materials*, American Chemical Society, Washington, DC, 1999; (f) M.J. Duer, *Introduction to Solid-State NMR Spectroscopy*, Blackwell Publishing, Oxford, 2004; (g) J. Blümel, *Nachr. Chem. Tech. Lab.* 54 (2006) 632.
- [10] S. Reinhard, J. Blümel, *Magn. Reson. Chem.* 41 (2003) 406.
- [11] (a) K.D. Behringer, J. Blümel, *Z. Naturforsch.* 50b (1995) 1723; (b) C. Merckle, J. Blümel, *Chem. Mater.* 13 (2001) 3617; (c) T. Posset, F. Rominger, J. Blümel, *Chem. Mater.* 17 (2005) 586; (d) S. Brenna, T. Posset, J. Furrer, J. Blümel, *Chem. Eur. J.* 12 (2006) 2880.
- [12] G. Tsiavaliaris, S. Haubrich, C. Merckle, J. Blümel, *Synlett* (2001) 391.
- [13] J. Blümel, *J. Am. Chem. Soc.* 117 (1995) 2112.
- [14] K.D. Behringer, J. Blümel, *J. Liq. Chromatogr.* 19 (1996) 2753.
- [15] K.D. Behringer, J. Blümel, *J. Chem. Soc., Chem. Commun.* (1996) 653.
- [16] (a) J. Blümel, *Inorg. Chem.* 33 (1994) 5050; (b) J. Sommer, Y. Yang, D. Rambow, J. Blümel, *Inorg. Chem.* 43 (2004) 7561.
- [17] F. Piestert, R. Fetouaki, M. Bogza, T. Oeser, J. Blümel, *Chem. Commun.* (2005) 1481.
- [18] T. Posset, J. Blümel, *J. Am. Chem. Soc.* 128 (2006) 8394.
- [19] (a) J. Stahl, J.C. Bohling, E.B. Bauer, T.B. Peters, W. Mohr, J.M. Martín-Alvarez, F. Hampel, J.A. Gladysz, *Angew. Chem., Int. Ed.* 41 (2002) 1871. *Angew. Chem.* 114 (2002) 1951; (b) A.J. Nawara, T. Shima, F. Hampel, J.A. Gladysz, *J. Am. Chem. Soc.* 128 (2006) 4962.
- [20] (a) N. Lewanzik, T. Oeser, J. Blümel, J.A. Gladysz, *J. Mol. Catal. A: Chem.* 254 (2006) 20; (b) E.B. Bauer, F. Hampel, J.A. Gladysz, *Organometallics* 22 (2003) 5567.
- [21] Program SADABS v2.03 for absorption correction: G.M. Sheldrick, Bruker Analytical X-ray Division, Madison, Wisconsin, 2001.
- [22] Software package SHELXTL v6.12 for structure solution and refinement: G.M. Sheldrick, Bruker Analytical X-ray Division, Madison, Wisconsin, 2001.
- [23] Program ORTEP-3 for Windows: L.J. Farrugia, *J. Appl. Crystallogr.* 30 (1997) 565.
- [24] A. Polas, J.D.E.T. Wilton-Ely, A.M.Z. Slawin, D.F. Foster, P.J. Steynberg, M.J. Green, D.J. Cole-Hamilton, *Dalton Trans.* (2003) 4669.
- [25] H.P. Lane, C.A. McAuliffe, R.G. Pritchard, *Acta Crystallogr., Sect. C* 48, *Cryst. Struct. Commun.* (1992) 2002.
- [26] (a) R.D. Holmes-Smith, R.D. Osei, S.R. Stobart, *J. Chem. Soc., Perkin Trans. I* (1983) 861; (b) F.L. Joslin, S.R. Stobart, *Inorg. Chem.* 32 (1993) 2221.
- [27] (a) R.K. Harris, *Can. J. Chem.* 42 (1964) 2275; (b) W.H. Hersh, P. Xu, B. Wang, J.W. Yom, C.K. Simpson, *Inorg. Chem.* 35 (1996) 5453; (c) W.H. Hersh, *J. Chem. Educ.* 74 (1997) 1485.